Two Novel $\{Ti_6P_2\}$ Clusters Decorated with Inorganic Acids①

ZHENG Ai-Ping[a, b] GAO Mei-Yan[b]
FANG Wei-Hui[b②] KANG Yao[b②]

[a] (*College of Chemistry, Fuzhou University, Fuzhou* 350100, *China*)

[b] (*State Key Laboratory of Structural Chemistry, Fujian Institute of Research on the Structure of Matter, Chinese Academy of Sciences, Fuzhou* 350002, *China*)

ABSTRACT Two inorganic acids decorating titanium-oxo clusters (PTCs), $Ti_6O_4(O^iPr)_{10}(O_3P\text{-}Phen)_2(NO_3)_2$ (**PTC-251**) and $Ti_6O_4(O^iPr)_{10}(O_3P\text{-}Phen)_2(HSO_4)_2$ (**PTC-252**) (H_2O_3P-Phen = phenylphosphinic acid) have been synthesized under solvothermal conditions. As a result of the labile coordination sites of the $\{Ti_6P_2\}$ unit, nitrite and sulfate adopt different capping mode. Besides, they also present different space packing. The photocatalytic H_2 evolution activities of these obtained PTCs have been studied, with sulfate decorating **PTC-252** presenting a maximum H_2 production rate up to 110.95 μmol g^{-1} h^{-1}.

Keywords: polyoxo-titanium clusters, inorganic acid, labile coordination sites, water-splitting;
DOI: 10.14102/j.cnki.0254–5861.2011–2853

1 INTRODUCTION

Nanoscale titanium oxide has been broadly used in solving energy crisis due to its abundance, low-cost, little toxicity, nice photostability, and high photocatalytic efficiency[1, 2]. However, it is difficult to determine the reaction mechanisms while utilized as photocatalysis. Hence, crystalline polyoxo titanium clusters (PTCs) with accurate structures have appealed to researchers, and a great number of crystalline PTCs have been synthesized and characterized recently[3-9]. One of the most important studies is bandgap engineering[10, 11]. And one method to reduce the bandgap of titanium oxo clusters and enhance their visible light adsorption is the organic ligand modification[12-15].

In the family of PTCs, organophosphate-stabilized $\{Ti_6P_2\}$ cluster with six labile coordination sites has been used as a platform for ligands substitution and metal incorporation[16-18]. For example, in 2014, Schubert *et al.* reported a series of stable $Ti_6O_4(O^iPr)_{10}(O_3PR)_2(OAc)_2$ (OAc = acetate) cluster with different phosphonate ligands[19]. Subsequently, our group used carboxylates, phosphonates and sulfonates ligands to replace the active coordination sites of $\{Ti_6P_2\}$ cluster, and demonstrated that high electron-withdrawing organic species can reduce the bandgaps of these complexes[20]. However, there are still no studies on the inorganic acid-modified $\{Ti_6P_2\}$ cluster. As is known to us all, inorganic acids like nitric or sulfuric acid are cheap, stable, and widely available. Thus, it is meaningful to study how inorganic acids occur in such $\{Ti_6P_2\}$ structure.

As a continuation of our effort, we researched constructing $\{Ti_6P_2\}$ cluster-based PTCs using nitric or sulfuric acid. Successfully, two complexes, namely, $Ti_6O_4(O^iPr)_{10}(O_3P\text{-}Phen)_2(NO_3)_2$ (**PTC-251**) and $Ti_6O_4(O^iPr)_{10}(O_3P\text{-}Phen)_2(HSO_4)_2$ (**PTC-252**) (H_2O_3P-Phen = phenylphosphinic acid), were synthesized and structurally characterized. As expected, the introduced inorganic acids indeed replace the organic carboxylates sites (like acetate, benzoic acid, *etc.*), and locate on the upper and bottom surfaces of $\{Ti_6P_2\}$ cluster. Moreover, the bandgap properties and photocatalytic water-splitting hydrogen-evolution activities of these two complexes are also investigated.

Received 17 April 2020; accepted 15 June 2020 (**CCDC 1995565 for 1 and 1995566 for 2**)

① This project was supported by National Natural Science Foundation of China (21771181, 21935010 and 21973096) and Youth Innovation Promotion Association CAS (2017345)

② Corresponding authors. E-mail: fwh@fjirsm.ac.cn and ky@fjirsm.ac.cn

2 EXPERIMENTAL

2. 1 Materials and measurements

All chemicals except distilled water were purchased commercially and used without further purification. Distilled water was obtained by our laboratory. $Ti(O^iPr)_4$ was purchased from Aladdin, and phenylphosphonic acid was purchased from Energy Chemical. Isopropyl alcohol, nitric acid and sulfuric acid were purchased from Sinopharm Chemical Reagent Beijing. Powder X-ray diffraction (PXRD) data were obtained by placing target crystals onto the flat sample holders using a MiniFlex2 X-ray diffractometer with Cu$K\alpha$ radiation (λ = 0.1542 nm) in the 2θ range from 5 ° to 50 ° with a scanning rate of 5 °/min. The Fourier transform infrared (FTIR) spectroscopic data (KBr pellets) were obtained on a PerkinElmer Spectrum 100 FTIR Spectrometer. The diffuse reflectance ultraviolet (UV) data were collected on powder samples with $BaSO_4$ as standard (100% reflectance) with a PerkinElmer Lamda-950 UV spectrophotometer at room temperature. Thermogravimetric analysis (TGA) was performed on a Mettler Toledo TGA/SDTA 851^e analyzer at a heating rate of 10 ℃/min from 25 to 600 ℃ under a nitrogen atmosphere.

2. 2 Synthesis

2. 2. 1 $Ti_6O_4(O^iPr)_{10}(O_3P\text{-}Phen)_2(NO_3)_2$ (PTC-251)

Phenylphosphonic acid (0.9941 g, 7.0 mmol) and 4 drops of nitric acid were mixed in 5.5 mL anhydrous isopropanol. And then $Ti(O^iPr)_4$ (0.92 mL, 3.0 mmol) was added rapidly into the mixture. The resultant solution was sealed and heated at 80 ℃ for 3 days. Colorless block crystals of **PTC-251** were obtained after cooling to room temperature (Yield: 53% based on $Ti(OiPr)_4$). Important IR data (KBr, cm^{-1}): 2970(m), 2932(w), 2864(w), 1627(w), 1555(s), 1474(w), 1438(w), 1366(w), 1275(s), 1034(m), 989(s), 928(m), 754(m), 684(m), 609(w), 551(w).

2. 2. 2 $Ti_6O_4(O^iPr)_{10}(O_3P\text{-}Phen)_2(HSO_4)_2$ (PTC-252)

PTC-252 was prepared by the same procedure as that for **PTC-251**, except the nitric acid was replaced by sulfuric acid. Colorless blocks crystals of **PTC-252** were obtained (60% yield based on $Ti(O^iPr)_4$). Important IR data (KBr, cm^{-1}): 2973(m), 2930(w), 2866(w), 2311(w), 1625(m), 1445(s), 1363(m), 1327(w), 1202(m), 1140(w), 1038(w), 993(vs), 939(w), 756(m), 693(s), 621(w), 548(m), 430(w).

2. 3 X-ray crystallography

The intensity crystallography data of **PTC-251** and **PTC-252** were collected on a Supernova and Xcalibur single crystal diffractometer with graphite-monochromatized Cu$K\alpha$ radiation (λ = 1.54178 Å) and Mo$K\alpha$ radiation (λ = 0.71073 Å), respectively. All absorption corrections were applied by using SADABS[21]. The structures were solved by direct methods and refined by full-matrix least-squares on F^2 with SHELXTL-2014 and OLEX-2 programs[22]. All atoms except hydrogen atoms were refined anisotropically while hydrogen atoms were generated geometrically. Crystal data for **PTC-251**: $C_{42}N_2O_{26}P_2Ti_6H_{80}$ (M_r = 1378.42 g/mol): orthorhombic, space group *Pbca* (No. 61), a = 16.9346(3), b = 17.4591(4), c = 22.3238(5) Å, V = 6600.3(2) Å^3, Z = 4, T = 293(2) K, μ(Cu$K\alpha$) = 6.984 mm^{-1}, D_c = 1.387 g/cm^3, 16721 reflections measured (7.92 ≤2θ≤148.58 °), 6624 unique (R_{int} = 0.0321, R_{sigma} = 0.0326) which were used in all calculations. The final R = 0.0685 ($I > 2\sigma(I)$) and wR = 0.2257 (all data). Crystal Data for **PTC-252**: $C_{42}H_{82}O_{28}P_2S_2Ti_6$ (M_r = 1448.53 g/mol): triclinic, space group $P\bar{1}$, a = 11.4280(10), b = 12.6293(18), c = 13.3326(14) Å, α = 118.223(13) °, β = 92.481(8) °, γ = 107.367(10) °, V = 1578.8(4) Å^3, Z = 1, T = 293(2) K, μ(Mo$K\alpha$) = 0.918 mm^{-1}, D_c = 1.524 g/cm^3, 11324 reflections measured (4.85 ≤2θ≤56.46 °), 6400 unique (R_{int} = 0.0293, R_{sigma} = 0.0538) which were used in all calculations. The final R = 0.0455 ($I > 2\sigma(I)$) and wR = 0.1198 (all data).

3 RESULTS AND DISCUSSION

3. 1 Crystal structures of PTC-251 and PTC-252

The organic modifications on {Ti_6P_2} cluster have been reported in 2014 and 2016[19, 20, 23]. Herein, it's the first time to decorate the {Ti_6P_2} cluster with different inorganic acids. The crystal belongs to monoclinic system with space group *Pbca*. {$Ti_3(\mu_3\text{-}O)$} subunit is a common and low-nuclearity moiety existing in the hydrolysis of titanium[24-26]. This fragment usually acts as a second building block generating larger aggregation[19, 27-33]. In **PTC-251**, such {$Ti_3(\mu_3\text{-}O)$} triangle block was equatorially bridged by isopropoxide groups (Fig. 1). Five isopropoxide ligands alternately adopted bridging bidentate and monodentate coordination mode. Axially, it was then linked by a nitrate to form $Ti_3(\mu_3\text{-}O)(\mu_2\text{-}O^iPr)_2(O^iPr)_3(NO_3)^{4+}$ ({Ti_3}). Two parallel {Ti_3} are connected through oxo bridges and phenylphosphinic ligands to form a {Ti_6P_2} cluster (Fig. 2). Ti1 and Ti2 ions in the {Ti_6P_2} core are six-coordinated whilst Ti3 is only five-coordinated.

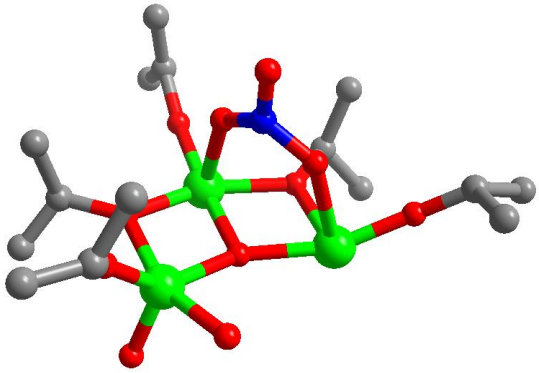

Fig. 1. Perspective view of the {$Ti_3(\mu_3$-O)} subunit in PTC-251. Color code: O red; C grey; Ti green; N blue

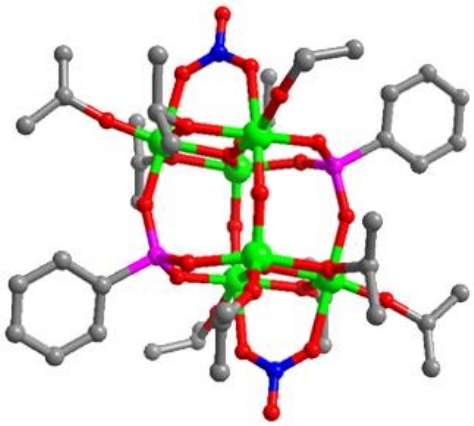

Fig. 2. Molecular structure of PTC-251. Color code: O red; C grey; Ti green; N blue

The cluster core of **PTC-252** is isostructural to that of **PTC-251**. However, the attachment of the "outer" Ti coordination environment is different. Sulfate took tridentate coordination mode capping on the {$Ti_3(\mu_3$-O)} subunit (Fig. 3). As a result, all of the Ti ions in **PTC-252** are in octahedral coordination geometry (Fig. 4). The Ti–O bond lengths between nitrate and sulfate were longer than the other Ti–O bond in the structure (Tables S1 and S2). These clusters packed differently largely attributed to the steric hindrance from the two outer faces (Fig. S1).

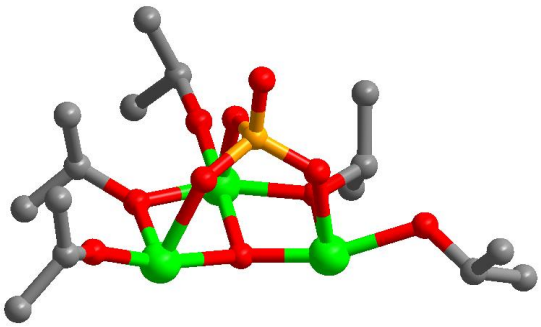

Fig. 3. Perspective view of the {$Ti_3(\mu_3$-O)} subunit in PTC-252. Color code: O red; C grey; Ti green; N blue

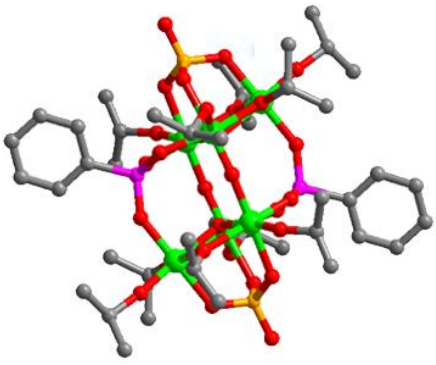

Fig. 4. Molecular structure of PTC-252. Color code: O red; C grey; Ti green; S orange

3. 2 Characterization

The experimental PXRD patterns of **PTC-251** and **PTC-252** are well-matched with their simulated PXRD patterns (Fig. S2), evidencing that the experimental samples are in good phase purity. The different reflection intensity between experimental and simulated is attributed to the

variation of the powder sample in the preferred orientation. The TGA of **PTC-251** and **PTC-252** was analyzed in a dry air atmosphere from 25 to 600 ℃ (Fig. S3). The TGA of **PTC-251** exhibits overall one-step weight loss while **PTC-252** undergoes two stages of weight loss. The UV absorption spectra of **PTC-251** and **PTC-252** present bandgaps of 3.39 and 3.34 eV, respectively (Fig. S4).

The IR spectra of **PTC-251** and **PTC-252** have been recorded in the range of 4000～400 cm^{-1} from solid samples palletized with KBr, which are presented in Fig. S5. In the high wavenumber region (v > 1000 cm^{-1}), the weak absorption bands at 3010～2910 cm^{-1} are observed, which can be ascribed to the stretching vibration modes of C–H bonds in O^iPr groups. The characteristic skeletal vibrations of benzene rings are observed at 1640～1430 cm^{-1}. Besides, the peaks appearing at 1430～1260 cm^{-1} and 1110～1040 cm^{-1} can be respectively assigned to the characteristic bending vibrations of δ_{C-H} and stretching vibration of ν_{C-O}. In the low wavenumber region (v < 1000 cm^{-1}), the absorptions in the region ca. 800～642 cm^{-1} can be attributed to the C–H in-plane or out-of-plane bends, ring breathing, and ring deformation absorptions of benzene rings. What's more, the characteristic vibration of inorganic acid can be also observed at 861～827 cm^{-1} for NO_3^- in **PTC-251**, 620～550 cm^{-1} for HSO_4^{2-} in **PTC-252**. Thus, the result of IR spectra coincides with that from the X-ray single-crystal structural analysis.

3. 3 Photocatalytic properties

To evaluate the photocatalytic performances of **PTC-251** and **PTC-252**, photocatalytic hydrogen production studies were carried out under UV-light. Although acetate decorating {Ti_6P_2} cluster didn't show any hydrogen evolution activities[20], **PTC-251** and **PTC-252** with efficient photocatalytic abilities in water-splitting hydrogen-evolution reactions can be observed. The nitrate decorating **PTC-251** gives the hydrogen production of 14.5 μmol g^{-1} h^{-1}, while the sulfate decorating **PTC-252** presents the higher hydrogen production of 110.95 μmol g^{-1} h^{-1}. The photocatalytic performance of **PTC-252** was comparable to some PTCs and metal organic frameworks[34, 35]. The rate trends of these two compounds are shown in Fig. 5. Especially to **PTC-252**, the steady H_2 evolution rate indicates that the {Ti_6P_2} cluster decorated by sulfate is quite stable. These results also confirm that the photocatalytic H_2 evolution activity of PTCs can be influenced by modified ligands.

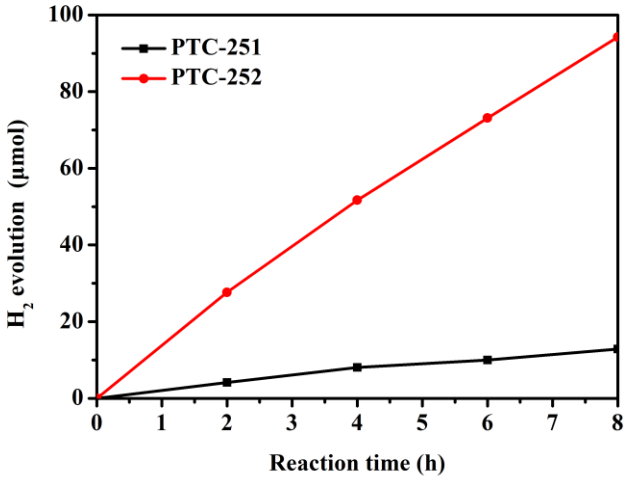

Fig. 5. Comparison of H_2 evolution behaviors under UV-vis light-driven with PTC-251 and PTC-252

4 CONCLUSION

In summary, we have successfully utilized {Ti_6P_2} clusters as a platform and constructed two inorganic acids decorating **PTC-251** and **PTC-252**. The coordination modes of capped inorganic acid on {Ti_6P_2} clusters are inconsistent, which leads to totally different supramolecular packing. Moreover, the photocatalytic H_2 evolution activities of these two PTCs are also different. The H_2 evolution rate of **PTC-252** can reach up to 110.95 μmol g^{-1} h^{-1} while that of **PTC-251** is only 14.5 μmol g^{-1} h^{-1}. Our results not only enrich structures of organophosphate-stabilized PTCs but also provide an interesting model for better understanding the structure-property relationships of Ti–O materials.

REFERENCES

(1) Chen, X.; Mao, S. S. Titanium dioxide nanomaterials: synthesis, properties, modifications, and applications. *Chem. Rev.* **2007**, 107, 2891–959.

(2) Chen, X.; Shen, S.; Guo, L.; Mao, S. S. Semiconductor-based photocatalytic hydrogen generation. *Chem. Rev.* **2010**, 110, 6503–6570.

(3) Rozes, L.; Sanchez, C. Titanium oxo-clusters: precursors for a lego-like construction of nanostructured hybrid materials. *Chem. Soc. Rev.* **2011**, 40, 1006–1030.

(4) Coppens, P.; Chen, Y.; Trzop, E. Crystallography and properties of polyoxotitanate nanoclusters. *Chem. Rev.* **2014**, 114, 9645–9661.

(5) Fang, W. H.; Zhang, L.; Zhang, J. Synthetic strategies, diverse structures and tuneable properties of polyoxo-titanium clusters. *Chem. Soc. Rev.* **2018**, 47, 404–421.

(6) Zhao, C.; Han, Y. Z.; Dai, S.; Chen, X.; Yan, J.; Zhang, W.; Su, H.; Lin, S.; Tang, Z.; Teo, B. K.; Zheng, N. Microporous cyclic titanium-oxo clusters with labile surface ligands. *Angew. Chem. Int. Ed.* **2017**, 56, 16252–16256.

(7) Zhang, G.; Liu, C.; Long, D. L.; Cronin, L.; Tung, C. H.; Wang, Y. Water-soluble pentagonal-prismatic titanium-oxo clusters. *J. Am. Chem. Soc.* **2016**, 138, 11097–11100.

(8) Zhang, G.; Li, W.; Liu, C.; Jia, J.; Tung, C. H.; Wang, Y. Titanium-oxide host clusters with exchangeable guests. *J. Am. Chem. Soc.* **2018**, 140, 66–69.

(9) Chakraborty, B.; Weinstock, I. A. Water-soluble titanium-oxides: complexes, clusters and nanocrystals. *Coord. Chem. Rev.* **2019**, 382, 85–102.

(10) Matthews, P. D.; King, T. C.; Wright, D. S. Structure, photochemistry and applications of metal-doped polyoxotitanium alkoxide cages. *Chem. Commun.* **2014**, 50, 12815–12823.

(11) Li, N.; Matthews, P. D.; Luo, H. K.; Wright, D. S. Novel properties and potential applications of functional ligand-modified polyoxotitanate cages. *Chem. Commun.* **2016**, 52, 11180–11190.

(12) Liu, C.; Hu, J.; Liu, W.; Zhu, F.; Wang, G.; Tong, C. H.; Wang, Y. Binding modes of salicylic acids to titanium-oxide molecular surfaces. *Chem. Eur. J.* **2020**, 26, 2666–2674.

(13) Wu, Y. Y.; Wang, P.; Wang, Y. H.; Jiang, J. B.; Bian, G. Q.; Zhu, Q. Y.; Dai, J. Metal-phenanthroline fused Ti_{17} clusters, a single molecular source for sensitized photoconductive films. *J. Mater. Chem. A* **2013**, 1, 9862–9868.

(14) Hou, J. L.; Weng, Y. G.; Liu, P. Y,; Cui, L. N.; Zhu, Q. Y.; Dai, J. Effects of the ligand structures on the photoelectric activities, a model study based on titanium-oxo clusters anchored with S-heterocyclic ligands. *Inorg. Chem.* **2019**, 58, 2736–2743.

(15) Fan, Y.; Li, M. H.; Duan, R. H.; Lu, R. H.; Cao, J. T.; Zou, G. D.; Jing, Q. S. Phosphonate-stabilized titanium-oxo clusters with ferrocene photosensitizer: structures, photophysical and photoelectrochemical properties, and DFT/TDDFT calculations. *Inorg. Chem.* **2017**, 56, 12775–12782.

(16) Chaumont, C.; Huen, E.; Huguenard, C.; Mobian, P.; Henry, M. Toward colored reticular titanium-based hybrid networks: evaluation of the reactivity of the $[Ti_8O_8(OOCCH_2But)_{16}]$ wheel with phenol, resorcinol and catechol. *Polyhedron* **2013**, 57, 70–76.

(17) Hong, K.; Chun, H. Nonporous titanium-oxo molecular clusters that reversibly and selectively adsorb carbon dioxide. *Inorg. Chem.* **2013**, 52, 9705–9707.

(18) Frot, T.; Marrot, J.; Sanchez, C.; Rozes, L.; Sassoye, C. $Ti_8O_{10}(OOCR)_{12}$ R = $CH(CH_3)_2$ and CCl_3 caboxylate titanium oxo-clusters: potential SBUs for the synthesis of metal-organic frameworks. *Z. Anorg. Allg. Chem.* **2013**, 639, 2181–2185.

(19) Czakler, M.; Artner, C.; Schubert, U. Acetic acid mediated synthesis of phosphonate-substituted titanium oxo clusters. *Eur. J. Inorg. Chem.* **2014**, 2014, 2038–2045.

(20) Liu, J. X.; Gao, M. Y.; Fang, W. H.; Zhang, L.; Zhang, J. Bandgap engineering of titanium-oxo clusters: labile surface sites used for ligand substitution and metal incorporation. *Angew. Chem. Int. Ed.* **2016**, 55, 5160–5165.

(21) Sheldrick G. M. *SADABS: Program for Area Detector Adsorption Correction.* Institute for Inorganic Chemistry. University of Göttingen, Germany **1996**.

(22) Sheldrick, G. M. *SHELXL-2014: Program for Crystal Structure Solution and Refinement.* University of Göttingen, Göttingen, Germany **2014**.

(23) Zhu, B. C.; Zhang, L.; Zhang, J. Arsanilic acid stabilizing titanium-oxo clusters with various core structures and light absorption behaviours. *Inorg. Chem. Commun.* **2017**, 86, 14–17.

(24) Day, V. W.; Eberspacher, T. A.; Chen, Y. W.; Hao, J. L.; Klemperer, W. G. Low-nuclearity titanium oxoalkoxides the trititanates $[Ti_3O](OPri)_{10}$ and $[Ti_3O](OPri)_9(OMe)$. *Inorg. Chim. Acta* **1995**, 229, 391–405.

(25) Senouci, A.; Yaakoub, M.; Huguenard, C.; Henry, M. Molecular templating using titanium(IV) (oxo)alkoxides and

titanium(IV) (oxo)aryloxides. *J. Mater. Chem.* **2004**, 14, 3215–3230.

(26) Boyle, T. J.; Tyner, R. P.; Alam, T. M.; Scott, B. L.; Ziller, J. W.; Potter, B. G. Implications for the thin-film densification of TiO_2 from carboxylic acid-modified titanium alkoxides. Syntheses, characterizations, X-ray structures of $Ti_3(\mu_3\text{-}O)(O_2CH)_2(ONep)_8$, $Ti_3(\mu_3\text{-}O)(O_2CMe)_2(ONep)_8$, $Ti_6(\mu_3\text{-}O)_6(O_2CCHMe_2)_6(ONep)_6$, $[Ti(\mu\text{-}O_2CCMe_3)(ONep)_3]_2$, and $Ti_3(\mu_3\text{-}O)(O_2CCH_2CMe_3)_2(ONep)_8$ (ONep = OCH_2CMe_3). *J. Am. Chem. Soc.* **1999**, 121, 12104–12112.

(27) Corden, J. P.; Errington, W.; Moore, P.; Partridge, M. G.; Wallbridge, H. Synthesis of di-, tri- and penta-nuclear titanium(iv) species from reactions of titanium(iv) alkoxides with 2,2[prime or minute]-biphenol (H_2L_1) and 1,1[prime or minute]-binaphthol (H_2L_2); crystal structures of $[Ti_3([\mu_2\text{-}OPri)_2(OPri)_8L_1]$, $[Ti_3(OPri)_6L_{13}]$, $[Ti_5(\mu_3\text{-}O)_2(\mu_2\text{-}OR)_2(OR)_6L_{14}]$ (R = OPri, OBun) and $[Ti_2(OPri)_4L_{22}]$. *Dalton Trans.* **2004**, 1846–1851.

(28) Pajot, N.; Papiernik, R.; Hubert-Pfalzgraf, L. G.; Vaissermann, J.; Parraud, S. Metal-assisted activation of the C–O bond of 2-hydroxyethylmethacrylate. Synthesis and molecular structure of $Ti_5(OPr^i)_9(\mu\text{-}OPr^i)(\mu,\eta^2\text{-}OC_2H_4O)(\mu_3,\eta^2\text{-}OC_2H_4O)_3(\mu_4,\eta^2\text{-}OC_2H_4O)$. *Chem. Commun.* **1995**, 1817–1819.

(29) Radtke, A.; Piszczek, P.; Muziol, T.; Wojtczak, A. The structural conversion of multinuclear titanium(IV) mu-oxo-complexes. *Inorg. Chem.* **2014**, 53, 10803–10810.

(30) Day, V. W.; Eberspacher, T. A.; Klemperer, W. G.; Park, C. W. Dodecatitanates: a new family of stable polyoxotitanates. *J. Am. Chem. Soc.* **1993**, 115, 8469–8470.

(31) Schmid, R.; Mosset, A.; Galy, J. New compounds in the chemistry of group 4 transition-metal alkoxides. Part 4. Synthesis and molecular structures of two polymorphs of $[Ti_{16}O_{16}(OEt)_{32}]$ and refinement of the structure of $[Ti_7O_4(OEt)_{20}]$. *Dalton Trans.* **1991**, 1999–2005.

(32) Campana, C. F.; Chen, Y.; Day, V. W.; Klemperer, W. G.; Sparks, R. A. Polyoxotitanates join the Keggin family: synthesis, structure and reactivity of $[Ti_{18}O_{28}H][OBut]_{17}$. *Dalton Trans.* **1996**, 691–702.

(33) Coppens, P.; Chen, Y.; Trzop, E. Crystallography and properties of polyoxotitanate nanoclusters. *Chem. Rev.* **2014**, 114, 9645–9661.

(34) Narayanam, N.; Fang, W. H.; Chintakrinda, K.; Zhang, L.; Zhang, J. Deep eutectic-solvothermal synthesis of titanium-oxo clusters protected by π-conjugated chromophores. *Chem. Commun*. **2017**, 53, 8078–8080.

(35) Assi, H.; Pardo Pérez, L. C.; Mouchaham, G.; Ragon, F.; Asalevich, M.; Guillou, N. N.; Martineau, C.; Chevreau, H.; Kapteijn, F.; Gascon, J.; Fertey, P.; Elkaim, E.; Serre, C.; Devic, T. Investigating the case of titanium(iv) carboxyphenolate photoactive coordination polymers. *Inorg. Chem.* **2016**, 55, 7192–7199.